J Surfact Deterg (2018)
DOI 10.1002/jsde.12050

ORIGINAL ARTICLE

Construction of pH-Responsive Supramolecular Assemblies Based on Dynamic Covalent Bonds for Tunable Drug Release

Panpan Sun[1] · Fei Lu[1] · Aoli Wu[1] · Yue Yin[1] · Lijuan Shi[2] · Liqiang Zheng[1]

Received: 20 October 2017 / Revised: 7 January 2018 / Accepted: 5 March 2018

Abstract In the present work, we propose a novel strategy for preparing supramolecular self-assemblies for pH-responsive drug delivery. In alkaline solutions, a novel supra-amphiphile can be fabricated by a cationic surfactant dodecyl[2-(4-formylphenoxy)ethyl] dimethylammonium bromide (C_{12}-CHO) and a drug molecule (isonicotinic acid hydrazide) via a dynamic covalent bond. The constructed supra-amphiphile can hierarchically self-assemble into ordered micelles, which facilitates its use for drug delivery. Interestingly, the supra-amphiphile can facilely disassemble under specific acidic conditions, which is convenient for controlled release of drugs. Thus, this ionic amphiphile-drug system paves a way for realizing pH-driven targeted drug release.

Keywords Dynamic covalent bond · pH-response · Supra-amphiphile · Micelles · Drug delivery

J Surfact Deterg (2018).

Introduction

Smart self-assemblies, a class of stimuli-responsive materials, have attracted considerable attention in recent decades in the fields of polymers, electronics, biotechnology, and medicine science (Chen et al., 2014; Chu, Dreiss, & Feng, 2013; Guragain, Bastakoti, Malgras, Nakashima, & Yamauchi, 2015; Liu, Wang, Xie, Ju, & Chu, 2016). The diverse response properties include pH, CO_2, temperature, magnetic, redox, ultrasound, light, and so on (Deng, Ma, & Xie, 2015; Kong, Tan, Zhao, & Yin, 2013; Men, Schlaad, Voelkel, & Yuan, 2014; Wang, Tan, Wang, Li, & Zhang, 2014; Xing et al., 2016; Yin, Liu, Wang, & Feng, 2015). In particular, pH-responsive self-assemblies have drawn much attention in terms of their potential application in controlled drug delivery in recent years (Fu, Sun, & Yan, 2015; Gao, Chan, & Farokhzad, 2010; Kamaly, Yameen, Wu, & Farokhzad, 2016; Mao et al., 2016).

Supra-amphiphiles with fascinating structures and unique properties have been widely studied in the field of smart materials (Dong et al., 2015; Kang, Tang, Cai, & Zhang, 2016; Wang, Wang, & Zhang, 2012; Yu, Jie, & Huang, 2015). In contrast to the complex synthesis of traditional covalent amphiphiles, such amphiphiles are assembled by a noncovalent bond and/or a dynamic covalent bond (Chi, Yu, Shao, Chen, & Huang, 2016; Ji et al., 2015; Kang, Cai, et al., 2016). A dynamic covalent bond, a type of responsive covalent bond, can be broken and reformed reversibly and quickly under specific conditions (Corbett et al., 2006). Abundant dynamic covalent bonds, including imine (Wang, Wu, Wang, & Zhang, 2014), disulfide (Yang, Chen, & Hu, 2014; Yang et al., 2015), oxime (Jin et al., 2011), acylhydrazone (Cao et al., 2015), ester (Hu et al., 2015; Huang et al., 2014), and acetal bonds (Louage et al., 2017), have been developed. The reversible and responsible nature of dynamic covalent bonds endows the supramolecular materials with tunable features and functions. For instance, Haldar, Bauri, Li, Faust, and De (2015) fabricated the pH-responsive self-healing polymer

✉ Liqiang Zheng
lqzheng@sdu.edu.cn

[1] Key Laboratory of Colloid and Interface Chemistry, Ministry of Education, Shandong University, Jinan, 250100, China

[2] Key Laboratory of Coal Science and Technology, Ministry of Education and Shanxi Province, Taiyuan University of Technology, Taiyuan, 030024, China

gels through imine (—HC═N—) bonds. Guo et al. (2017) obtained a multisensitive and self-healing hydrogel based on boronic ester and disulfide linkages. You's group investigated the dynamic covalent assemblies for the selective sensing of both Cu^{2+} and CN^- in water (Zha & You, 2016).

Generally, the imine and ester bonds are the most investigated pH-responsive dynamic covalent bonds in the field of smart self-assemblies. The formed pH-responsive assemblies have been used to preferentially release drugs at the sites of disease. Huang et al. (2014) successfully synthesized an amphiphilic drug–drug conjugate *via* a hydrolyzable ester linkage for cancer therapy. Xu et al. (2014) designed a PEG-DOX-Cur cancer prodrug through a Schiff base linker, which can reduce the proportion of inactive materials and minimize drug leakage. As a special type of imine, a dynamic acylhydrazone bond, which is formed via the condensation of hydrazides with carbonyl groups, is more stable than most ordinary imines, which is beneficial for drug delivery in the complex environment of a living body. For instance, Zhong's group introduced the acylhydrazone bond into the PEG-g-DOX prodrug nanoparticles for targeted cancer chemotherapy (Zhou et al., 2011). In some degree, the drug carriers are confined to the polymer-drug delivery, due to which the drug-loading capacity is somewhat low. The small molecule amphiphile-drug systems, which are expected to provide a new way to construct an effective drug delivery and loading system, have rarely been investigated so far.

Herein, we designed and constructed a pH-responsive supra-amphiphile Dodecyl[2-(4-benzoylhydrazone isonicotinic acid hydrazide)ethyl] dimethylammonium bromide, (C_{12}-CHIM) by connecting a single-tailed ionic surfactant (C_{12}-CHO) with a drug molecule (isonicotinic acid hydrazide [IAH]) through a dynamic covalent bond. Our aim is to investigate the self-assembly and disassembly of C_{12}-CHIM and realize the tunable release of carried drug using this reversible supramolecular system as shown in Scheme 1.

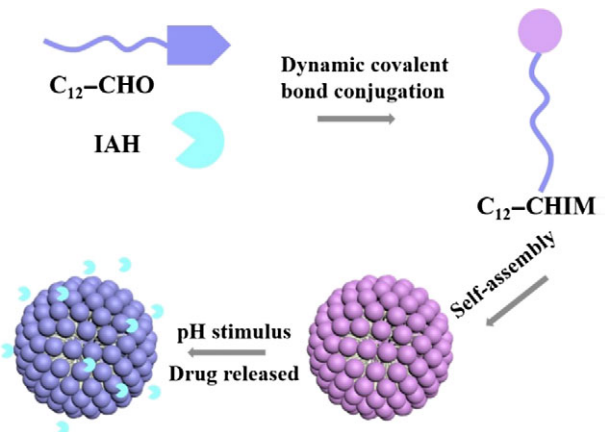

Scheme 1 Schematic illustration of the supra-amphiphile and its application in tunable drug release

Experimental

Materials and Synthesis

4-Hydroxybenzaldehyde (99%), 1,2-dibromoethane (99%), IAH (98%), and *N*,*N*-dimethyldodecylamine (97%) were purchased from J&K Scientific Ltd (Shanghai, China). $CDCl_3$ (99.96%) and D_2O (99.96%) were obtained from Sigma–Aldrich (Shanghai, China). Diethyl ether, CH_2Cl_2, CH_3CN, PE (petroleum ether) $MgSO_4$, KOH, and *n*-hexane were obtained from Shanghai Chemical Co (Shanghai, China). All the materials were used as received without any purification. Deionized water was used throughout all the experiments.

Synthesis of 4-(2-Bromoethoxy) Benzaldehyde

The synthesis route is shown in Scheme 2 (Ma et al., 2014; Santra, Mukherjee, Bej, Saha, & Ghosh, 2015; Takakura et al., 2014). 4-Hydroxybenzaldehyde (1 g, 8.2 mmol), 1,2-dibromoethane (3.85 g, 20.5 mmol), and K_2CO_3 (3.40 g, 24.6 mmol) were dissolved in CH_3CN (80 mL), and then the mixture was refluxed with stirring for 24 h. After the reaction, the solvent was removed under reduced pressure to yield a wheat-colored solid. The solid was dissolved in CH_2Cl_2, dried over anhydrous $MgSO_4$, and filtered. The solvent was removed under reduced pressure. The crude product was purified by column chromatography (silica gel, CH_2Cl_2:PE = 3:2, v/v) to yield compound **A** as a white solid. ^{1}H nuclear magnetic resonance spectroscopy (NMR) (300 MHz, $CDCl_3$): δ 3.67 (t, 2H), 4.38 (t, 2H), 7.04 (d, 2H), 7.89 (d, 2H), 9.90 (s, 1H). ^{13}C NMR (300 MHz, D_2O): δ_C (ppm) 31.53, 68.57, 115.51, 130.43, 132.30, 163.27, and 191.80. Mp, 52–58°C. ($[C_9H_9BrO_2 + H]^+$) m/z = 228.9859, found m/z = 228.9836.

Synthesis of B (C_{12}-CHO)

Compound **A** (1 g, 4.4 mmol) was dissolved in *N*,*N*-dimethyldodecylamine (5 mL) and the solution was heated at 80°C for 24 h. The reaction mixture was washed with diethyl ether at room temperature and the resulting powder was further washed with *n*-hexane to afford the amhiphilic aldehyde C_{12}-CHO as a light yellow solid. ^{1}H NMR (300 MHz, D_2O): δ_H (ppm) 0.86 (t, 3H), 1.14 (m, 18H), 1.60 (m, 2H), 3.08 (s, 6H), 3.18 (t, 2H), 3.63 (t, 2H), 4.34 (t, 2H), 6.74 (d, 2H), 7.50 (d, 2H), 9.51 (s, 1H). ^{13}C NMR (300 MHz, D_2O): δ_C (ppm) 13.9, 22.7–32.04, 52.44, 61.34, 62.35, 64.29, 114.76, 130.08, 132.09, 162.22, and 192.18. Mp, 43–80°C. ($[C_{23}H_{40}NO_2]^+$) m/z = 362.3053, found m/z 362.3127.

Critical Aggregation Concentration Measurement

A series of samples with different concentrations were prepared at the same pH (11.8 ± 0.2). Surface tension

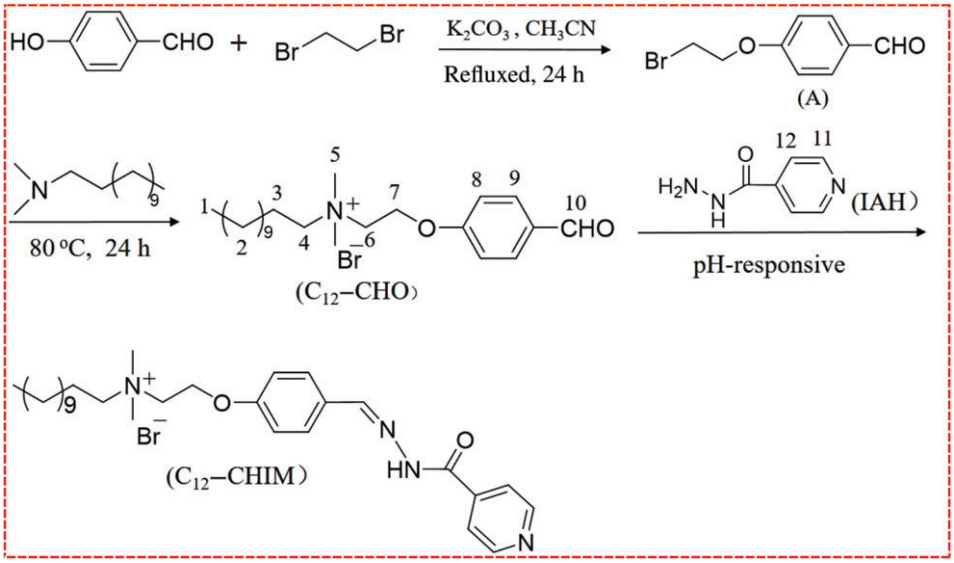

Scheme 2 Constructing route of C_{12}-CHIM

measurements were carried out on a model JYW-200B tensiometer (Chengde Dahua Instrument Co., Ltd. [Chengde, China], accuracy ±0.1 mN m^{-1}) using the ring method. The temperature was controlled using a thermostatic bath with an accuracy of 25 ± 0.1°C. Each sample was equilibrated for 15 min and all measurements were repeated at least three times until the values became reproducible.

Dynamic Light Scattering

The micelle size distributions of the micelles were determined by dynamic light scattering (DLS) using a Nanotrac Particle Size Analyzer (Nanotrac NPA 250 [Malvern, Britain]) and the microtrac FLEX application software program (Florida, USA). All measurements were carried out using a laser diode (780 nm wavelength, 3 mW nominal, and Class IIIB at a scattering angle of 180°). The temperature was controlled using a thermostat (F31C; Julabo [Seelbach, Germany]) with an accuracy of 25 ± 0.1°C.

^{1}H NMR Analysis at Different pH Values

^{1}H NMR spectra were recorded on a Bruker Advance 300 spectrometer (Rheinstetten, Germany) equipped with a pulse field gradient module (Z axis) using a 5 mm broadband observe (BBO) probe. The instrument was run at a frequency of 300.13 MHz at 25 ± 0.1°C. For the NMR test, the solvent was D_2O, which was buffered by NaH_2PO_4, Na_2HPO_4, and Na_3PO_4. A series of samples at different pH values were prepared.

UV–Vis Spectroscopy

The UV–vis spectroscopy measurements for a series of samples at different pH values were carried out on a UV-4100 spectrophotometer (Hitachi, Tokyo, Japan). The buffer solutions were utilized as a blank in the experiments.

Transmission Electron Microscopy

Transmission electron microscopy (TEM) studies were performed with a Hitachi (Tokyo, Japan) 100CX-II TEM operating at 100 kV. A little of the sample solution (0.5 mg mL^{-1}) was sprayed onto the carbon-coated copper grid and negatively stained with a drop of 0.2 wt% phosphotungstic acid aqueous solution. The excess solution was wicked away carefully by touching the grid edge with a filter paper wedge.

Fourier Transform Infrared Spectroscopy (FTIR) Spectra

FTIR spectra were obtained using a PerkinElmer (Waltham, USA) spectrum two FTIR spectrometer in the range of 4000–450 cm^{-1}.

Results and Discussion

Construction of a Supra-Amphiphile by a Dynamic Covalent Bond

A functional supra-amphiphile was fabricated based on a dynamic covalent bond using the amphiphile C_{12}-CHO and

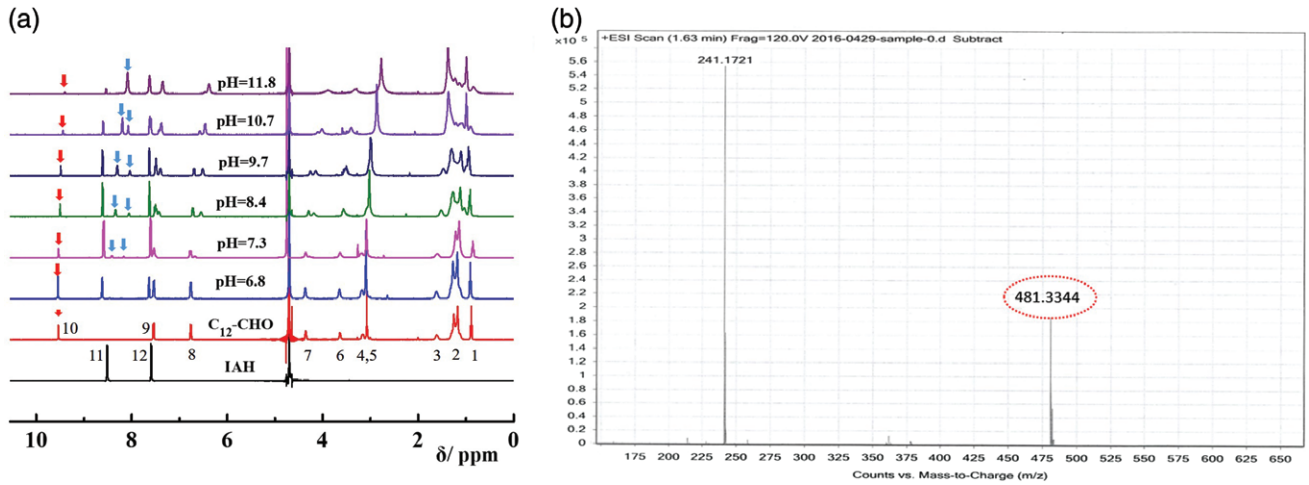

Fig. 1 (**a**) The ^{1}H NMR spectra of the mixture of equimolar C_{12}-CHO and IAH at different pH values at 298 K. The concentrations of all the samples are 6.0 mmol L^{-1} in D_2O; (**b**) mass analysis of the mixture of equimolar C_{12}-CHO and IAH at pH 11.8

the drug molecule IAH. The powerful evidence of pH-responsive complexation between C_{12}-CHO and IAH was provided by ^{1}H NMR. In general, the proton of aldehyde appears at about 9.5 ppm (red arrows in Fig. 1a) and there is no peak signal of the amino group in the aqueous solutions. As can be seen from Fig. 1a, the aldehyde peak declines and even disappears with increasing pH values and new peaks appear around 8.0 ppm (light blue arrows), indicating the formation of the acylhydrazone bond (Wang, Wang, Wang, & Zhang, 2011, 2012).

In general, the chemical shifts of protons on the surfactants move downfield during aggregation in the absence of any other specific interaction. Obviously, the protons of C_{12}-CHO move upfield slightly during the formation of a dynamic imine bond except for the protons on the terminal alkyl chain (C-1). This observed trend can be explained by the fact that the part of benzene ring would penetrate into the hydrophobic regions. The insertion of the benzene ring brings a more significant shielding effect to the protons on the alkyl chain due to the circular current effect. The upfield shifts of alkyl chain protons can be attributed to the shielding effect. The protons of IAH gradually shift downfield with the formation of an imine bond, indicating that more and more IAH molecules were inserted into the hydrophobic regions and more and more IAH molecules were involved in the aggregation of amphiphiles. Interestingly, the signal of the acylhydrazone bond presents two peaks at low pH values, which may be caused by the coexistence of two different aggregates in the transition stage (Yu, Tian, Fan, Ji, & Wang, 2012). One kind of aggregate

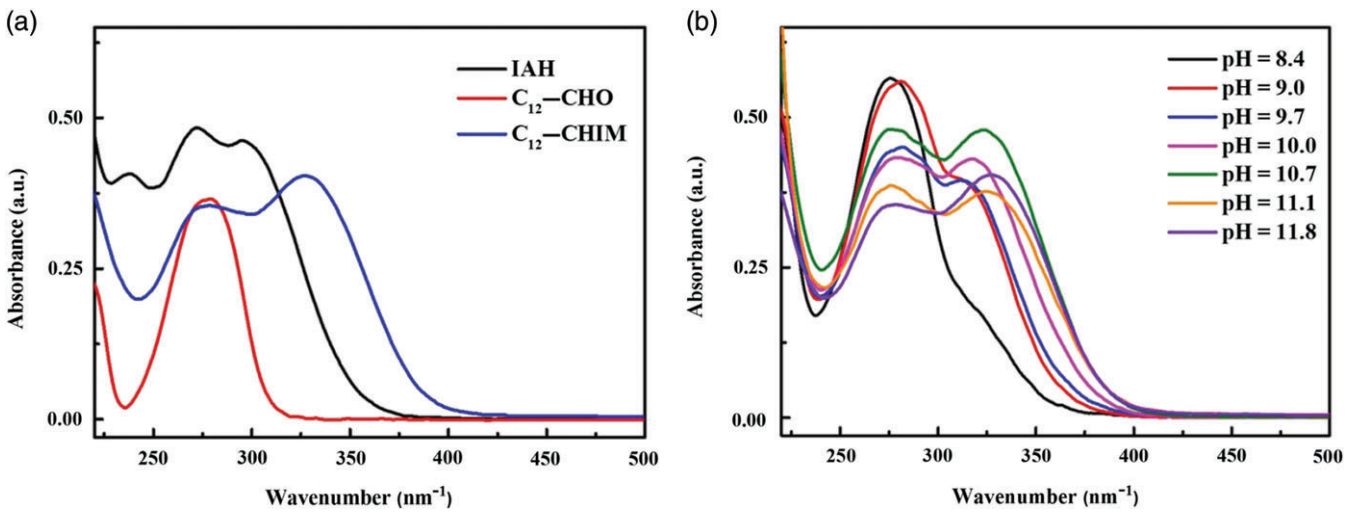

Fig. 2 UV–vis spectra of IAH, C_{12}-CHO, and C_{12}-CHIM at pH 11.8 (**a**) and the mixture of equimolar C_{12}-CHO and IAH at different pH values (**b**) at 298 K

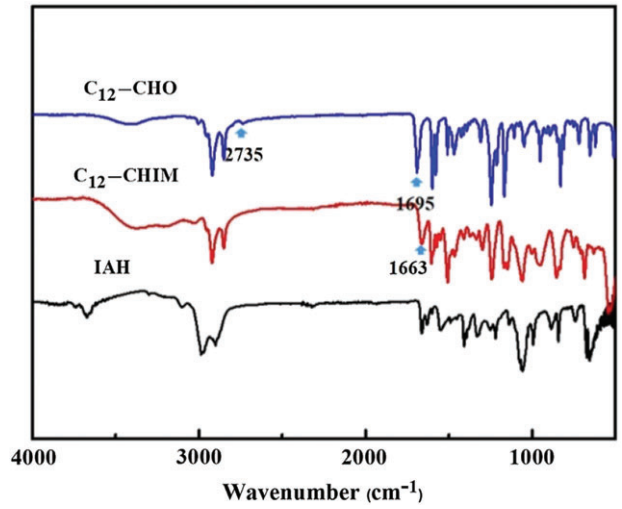

Fig. 3 FTIR spectra of C_{12}-CHO, IAH, and C_{12}-CHIM

is probably formed by the mixture of C_{12}-CHO and C_{12}-CHIM. Another kind of aggregate may be constituted by only C_{12}-CHIM. When the pH approaches 11.8, the aldehyde peak disappears and the two imine peaks are fused into one, further confirming the approximately complete conversion from C_{12}-CHO to C_{12}-CHIM. Additionally, the mass spectrometry (MS) analysis shows that the *m*/*z* ratio of C_{12}-CHIM is 481.3344 (Fig. 1b), which is in accordance with the calculated *m*/*z* ratio of 481.6854, further verifying the successful formation of C_{12}-CHIM by a dynamic covalent bond.

The formation of the acylhydrazone bond was also characterized using UV–vis spectrophotometry (Wu et al., 2014). As can be seen from Fig. 2a, the two adsorption peaks appear at about 270 and 340 nm when C_{12}-CHIM is formed. These peaks are attributed to the π–π* and *n*–π*

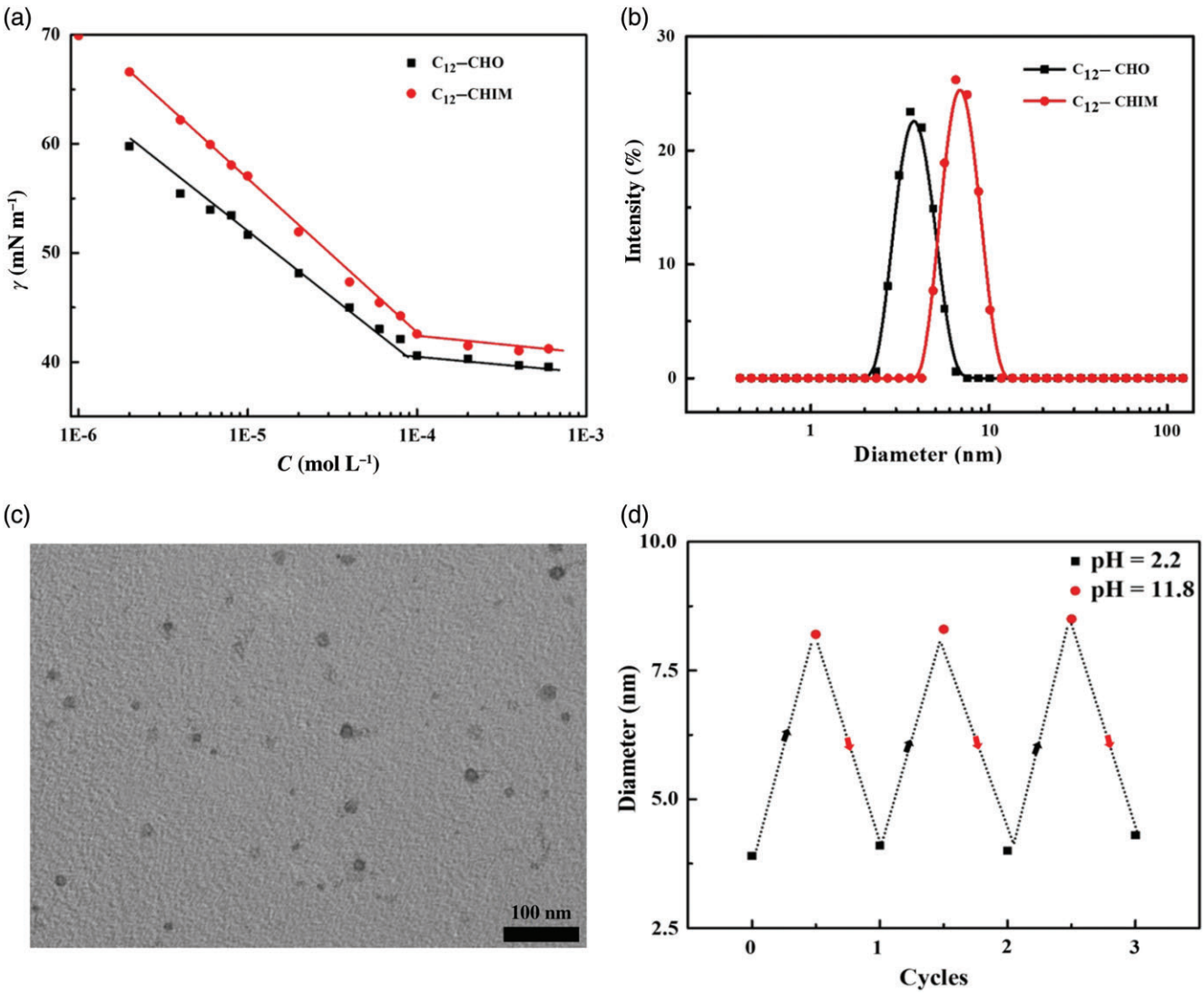

Fig. 4 (**a**) Surface tension as a function of concentration of C_{12}-CHO and C_{12}-CHIM; (**b**) DLS distribution of the C_{12}-CHO and C_{12}-CHIM nanoaggregates in aqueous solution (pH 11.8) at 298 K; (**c**) the TEM image of the aggregates of C_{12}-CHIM in aqueous solution (pH 11.8) at 6 mM (negatively stained with a 0.2 wt% phosphotungstic acid solution); and (**d**) DLS distributions measured over repeated cycles of adding base and acid

transition of the C═N bond in the acylhydrazone bond formed during the reaction between the acylhydrazone group in IAH and the aldehyde group in C_{12}-CHO. Meanwhile, compared to the adsorption of bulk IAH, a red shift from 295 to 328 nm can be seen from the adsorption of C_{12}-CHIM, as shown in the (Table 1), which is attributed to the enhanced conjugative effect after the combination of IAH and C_{12}-CHO. Simultaneously, acylhydrazone bond formation relying on pH was further proved in Fig. 2b. This is the first time the UV–vis method was used to follow the formation degree of a dynamic covalent bond. The maximum adsorption of the mixture of IAH and C_{12}-CHO is similar to that of C_{12}-CHO at pH 8.4. With increasing pH, a new adsorption at 328 nm appears and a gradual red shift occurs, confirming that the basic environment facilitates the formation of the acylhydrazone bond. FTIR analysis further verified the successful construction of C_{12}-CHIM. As can be seen in Fig. 3, the characteristic peaks at 2735 and 1695 cm^{-1} belong to the vibration frequencies of CH and C═O in the aldehyde group. In the FTIR spectrum of C_{12}-CHIM, the stretching absorption bond at 2735 cm^{-1} disappears and the vibration frequency of C═N at 1663 cm^{-1} appears, which further indicate the successful conjugation of C_{12}-CHO and IAH.

Revolution of Supramolecular Self-Assemblies *Via* pH-Stimulus

After the successful construction of amphiphile-drug complexes, we further explored the self-assembly behavior of C_{12}-CHIM in aqueous solutions. C_{12}-CHIM is still considered as an amphiphilic molecule that contains a long hydrophobic alkyl chain and a hydrophilic ammonium unit. The

Table 1 The wavenumber of the UV–vis spectra of the mixture of equimolar C_{12}-CHO and IAH at different pH values

pH	8.4	9.0	9.7	10.0	10.7	11.1	11.8
λ_{max} (nm)	Null	307	312	318	324	327	328

critical aggregation concentration (CAC) of C_{12}-CHIM is calculated to be about 0.10 mM using the surface tension method, while the CAC of C_{12}-CHO is about 0.085 mM (Fig. 4a), indicating that the hydrophilicity of C_{12}-CHIM is higher than C_{12}-CHO. It is probably because the conjunction of suprahydrophilic IAH enhanced the solubility of supra-amphiphiles. As shown in Fig. 4b, the aggregate sizes of C_{12}-CHO and C_{12}-CHIM are 3.9 and 8.2 nm, respectively. Compared with C_{12}-CHO, the increased aggregate size of C_{12}-CHIM further convinces the formation of the acylhydrazone bond. Thus, the molecular sizes of the supra-amphiphiles (C_{12}-CHIM) formed are larger than those of C_{12}-CHO.

TEM was used to visualize the nanostructure of assemblies. Fig. 4c presents spherical aggregates with sizes about 10–20 nm, which are larger than that measured using DLS. This is probably due to the coverage of aggregates by the staining agent. Interestingly, the pH-responsive self-assembly behavior is reversible when the pH values are cyclically increased and decreased. As shown in Fig. 4d, the aggregate size of the pH-sensitive system can still retain its initial value after being switched three times.

Application of Supramolecular Assemblies in Tunable Drug Release

Release of IAH from C_{12}-CHIM by the hydrolysis of the dynamic covalent bond was evaluated using UV–vis

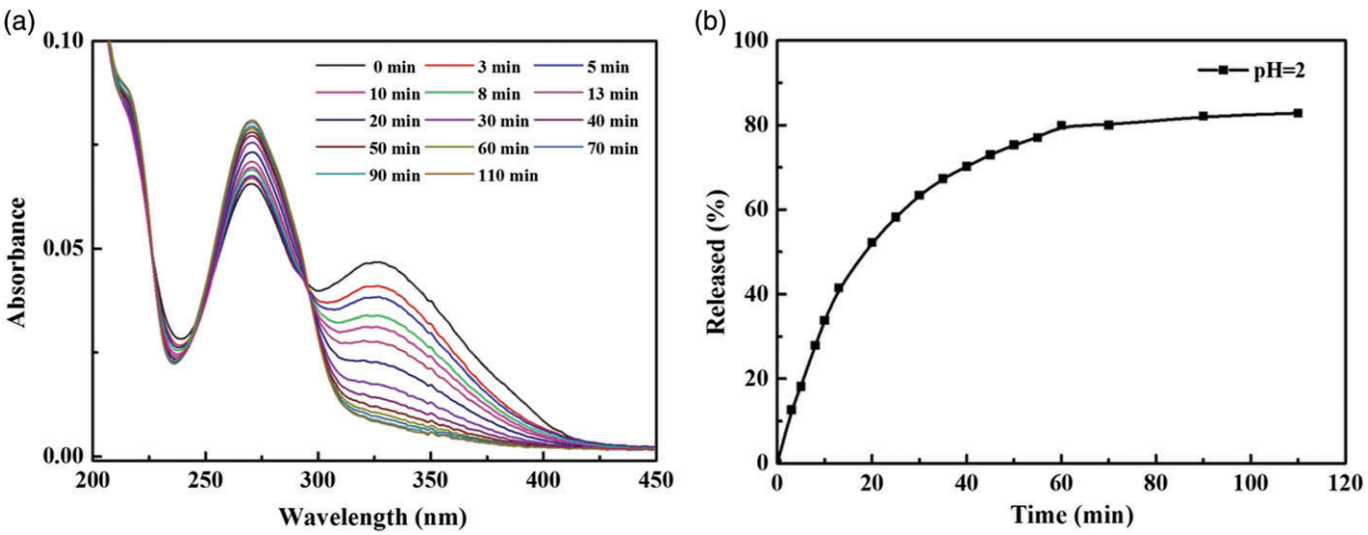

Fig. 5 (**a**) Dynamic UV–vis spectra at pH 2 and (**b**) released kinetic profiles of C_{12}-CHIM at pH 2 assayed using UV spectroscopy

spectroscopy (Wu et al., 2014). The time course of variation of UV–vis adsorption at pH 2 is depicted in Fig. 5a. The degradation of the acylhydrazone bond with time is reflected by the decrease of the absorption at 328 nm, which can also respond to the drug release rate (Fig. 5b). It is obvious that about 80% drug molecules can be released from the supramolecular aggregates within 120 min. Thus, these supramolecular assemblies can act as a drug delivery system, which can realize the controlled drug release by tuning the releasing environment.

Conclusion

In summary, we successfully synthesized a cationic surfactant (dodecyl[2-(4-formylphenoxy)ethyl] dimethylammonium bromide [C_{12}-CHO]) and constructed a supra-amphiphile (C_{12}-CHIM) by connecting the ionic surfactant C_{12}-CHO with the drug molecule IAH *via* a dynamic covalent bond. The supra-amphiphile can hierarchically self-assemble into stable micelles in alkaline buffered solutions, which facilitated the drug delivery. Interestingly, after the hydrolysis of the dynamic covalent bond in acidic environments, controlled drug release can be realized. Thus, this work paves a way for the regulated drug delivery of a supramolecular amphiphile-drug system.

Acknowledgements This work was supported by the National Natural Science Foundation of China (nos. 21573132 and 21403151), the National Basic Research Program (no. 2013CB834505), and the Natural Science Foundation for Young Scientists of Shanxi Province (no. 2016021045).

References

Cao, Y., Li, Y., Hu, X., Zou, X., Xiong, S., Lin, C., & Wang, L. (2015) Supramolecular nanoparticles constructed by DOX-based prodrug with water-soluble pillar [6]arene for self-catalyzed rapid drug release. *Chemistry of Materials*, **27**:1110–1119.

Chen, L., Zhao, G., Jiang, B., Sun, B., Wang, M., Xu, L., … Yang, H. (2014) Smart stimuli-responsive spherical nanostructures constructed from supramolecular metallodendrimers via hierarchical self-assembly. *Journal of the American Chemical Society*, **136**: 5993–6001.

Chi, X., Yu, G., Shao, L., Chen, J., & Huang, F. (2016) A dual-thermoresponsive gemini-type supra-amphiphilic macromolecular [3]pseudorotaxane based on pillar[10]arene/paraquat cooperative complexation. *Journal of the American Chemical Society*, **138**: 3168–3174.

Chu, Z., Dreiss, C., & Feng, Y. (2013) Smart wormlike micelles. *Chemical Society Reviews*, **42**:7174–7203.

Corbett, P., Leclaire, J., Vial, L., West, K., Wietor, J., Sanders, J., & Otto, S. (2006) Dynamic combinatorial chemistry. *Chemical Reviews*, **106**:3652–3711.

Deng, B., Ma, P., & Xie, Y. (2015) Reduction-sensitive polymeric nanocarriers in cancer therapy: A comprehensive review. *Nanoscale*, **7**:12773–12795.

Dong, R., Zhou, Y., Huang, X., Zhu, X., Lu, Y., & Shen, J. (2015) Functional supramolecular polymers for biomedical applications. *Advanced Materials*, **27**:498–526.

Fu, L., Sun, C., & Yan, L. (2015) Galactose targeted pH-responsive copolymer conjugated with near infrared fluorescence probe for imaging of intelligent drug delivery. *ACS Applied Materials & Interfaces*, **7**:2104–2115.

Gao, W., Chan, J., & Farokhzad, O. (2010) pH-responsive nanoparticles for drug delivery. *Molecular Pharmaceutics*, **7**:1913–1920.

Guo, R., Su, Q., Zhang, J., Dong, A., Lin, C., & Zhang, J. (2017) Facile access to multisensitive and self-healing hydrogels with reversible and dynamic boronic ester and disulfide linkages. *Biomacromolecules*, **18**:1356–1364.

Guragain, S., Bastakoti, B., Malgras, V., Nakashima, K., & Yamauchi, Y. (2015) Multi-stimuli-responsive polymeric materials. *Chemistry—A European Journal*, **21**:13164–13174.

Haldar, U., Bauri, K., Li, R., Faust, R., & De, P. (2015) Polyisobutylene-based pH-responsive self-healing polymeric gels. *ACS Applied Materials & Interfaces*, **7**:8779–8788.

Hu, M., Huang, P., Wang, Y., Su, Y., Zhou, L., Zhu, X., & Yan, D. (2015) Synergistic combination chemotherapy of camptothecin and floxuridine through self-assembly of amphiphilic drug–drug conjugate. *Bioconjugate Chemistry*, **26**:2497–2506.

Huang, P., Wang, D., Su, Y., Huang, W., Zhou, Y., Cui, D., … Yan, D. (2014) Combination of small molecule prodrug and nanodrug delivery: Amphiphilic drug–drug conjugate for cancer therapy. *Journal of the American Chemical Society*, **136**:11748–11756.

Ji, X., Shi, B., Wang, H., Xia, D., Jie, K., Wu, Z., & Huang, F. (2015) Supramolecular construction of multifluorescent gels: Interfacial assembly of discrete fluorescent gels through multiple hydrogen bonding. *Advanced Materials*, **27**:8062–8066.

Jin, Y., Song, L., Su, Y., Zhu, L., Pang, Y., Qiu, F., … Zhu, X. (2011) Oxime linkage: A robust tool for the design of pH-sensitive polymeric drug carriers. *Biomacromolecules*, **12**:3460–3468.

Kamaly, N., Yameen, B., Wu, J., & Farokhzad, O. (2016) Degradable controlled-release polymers and polymeric nanoparticles: Mechanisms of controlling drug release. *Chemical Reviews*, **116**: 2602–2663.

Kang, Y., Cai, Z., Tang, X., Liu, K., Wang, G., & Zhang, X. (2016) An amylase-responsive bolaform supra-amphiphile. *ACS Applied Materials & Interfaces*, **8**:4927–4933.

Kang, Y., Tang, X., Cai, Z., & Zhang, X. (2016) Supra-amphiphiles for functional assemblies. *Advanced Functional Materials*, **26**: 8920–8931.

Kong, Y., Tan, R., Zhao, L., & Yin, D. (2013) L-Proline supported on ionic liquid-modified magnetic nanoparticles as a highly efficient and reusable organocatalyst for direct asymmetric aldol reaction in water. *Green Chemistry*, **15**:2422–2433.

Liu, Z., Wang, W., Xie, R., Ju, X., & Chu, L. (2016) Stimuli-responsive smart gating membranes. *Chemical Society Reviews*, **45**:460–475.

Louage, B., Steenbergen, M., Nuhn, L., Risseeuw, M., Karalic, I., Winne, J., … De Geest, B. (2017) Micellar paclitaxel-initiated RAFT polymer conjugates with acid-sensitive behavior. *ACS Macro Letters*, **6**:272–276.

Ma, J., Cui, X., Wang, F., Wu, X., Zhao, J., & Li, X. (2014) Photoswitching of the triplet excited state of diiodobodipydithienylethene triads and application in photo-controllable triplet–triplet annihilation upconversion. *The Journal of Organic Chemistry*, **79**: 10855–10866.

Mao, J., Li, Y., Wu, T., Yuan, C., Zeng, B., Xu, Y., & Dai, L. (2016) A simple dual-pH responsive prodrug-based polymeric micelles for drug delivery. *ACS Applied Materials & Interfaces*, **8**: 17109–17117.

Men, Y., Schlaad, H., Voelkel, A., & Yuan, J. (2014) Thermoresponsive polymerized gemini dicationic ionic liquid. *Polymer Chemistry*, **5**:3719–3724.

Santra, S., Mukherjee, S., Bej, S., Saha, S., & Ghosh, P. (2015) Amino-ether macrocycle that forms Cu^{II} templated threaded heteroleptic complexes: A detailed selectivity, structural and theoretical investigations. *Dalton Transactions*, **44**:15198–15211.

Takakura, K., Yamamoto, T., Kurihara, K., Toyota, T., Ohnumad, K., & Sugawara, T. (2014) Spontaneous transformation from micelles to vesicles associated with sequential conversions of comprising amphiphiles within assemblies. *Chemical Communications*, **50**:2190–2192.

Wang, C., Wang, Z., & Zhang, X. (2012) Amphiphilic building blocks for self-assembly: From amphiphiles to supra-amphiphiles. *Accounts of Chemical Research*, **45**:608–618.

Wang, G., Wang, C., Wang, Z., & Zhang, X. (2011) Bolaform superamphiphile based on a dynamic covalent bond and its self-assembly in water. *Langmuir*, **27**:12375–12380.

Wang, G., Wang, C., Wang, Z., & Zhang, X. (2012) H-shaped supra-amphiphiles based on a dynamic covalent bond. *Langmuir*, **28**:14567–14572.

Wang, G., Wu, G., Wang, Z., & Zhang, X. (2014) Asymmetric and symmetric bolaform supra-amphiphiles: Formation of imine bond influenced by aggregation. *Langmuir*, **30**:1531–1535.

Wang, H., Tan, B., Wang, J., Li, Z., & Zhang, S. (2014) Anion-based pH responsive ionic liquids: Design, synthesis, and reversible self-assembling structural changes in aqueous solution. *Langmuir*, **30**:3971–3978.

Wu, X., Yu, G., Luo, C., Maeda, A., Zhang, N., Sun, D., … Lu, Z. (2014) Synthesis and evaluation of a nanoglobular dendrimer 5-aminosalicylic acid conjugate with a hydrolyzable Schiff base spacer for treating retinal degeneration. *ACS Nano*, **8**:153–161.

Xing, P., Chen, H., Ma, M., Xu, X., Hao, A., & Zhao, Y. (2016) Light and cucurbit [7]uril complexation dual-responsiveness of a cyanostilbene-based self-assembled system. *Nanoscale*, **8**: 1892–1896.

Xu, Z., Zhang, K., Hou, C., Wang, D., Liu, X., Guan, X., … Zhang, H. (2014) A novel nanoassembled doxorubicin prodrug with a high drug loading for anticancer drug delivery. *Journal of Materials Chemistry B*, **2**:3433–3437.

Yang, D., Chen, W., & Hu, J. (2014) Design of controlled drug delivery system based on disulfide cleavage trigger. *The Journal of Physical Chemistry B*, **118**:12311–12317.

Yang, Q., Tan, L., He, C., Liu, B., Xu, Y., Zhu, Z., … Shen, Y. (2015) Redox-responsive micelles self-assembled from dynamic covalent block copolymers for intracellular drug delivery. *Acta Biomaterialia*, **17**:193–200.

Yin, H., Liu, H., Wang, W., & Feng, Y. (2015) CO_2-induced reversible dispersion of graphene by a melamine derivative. *Langmuir*, **31**:12260–12267.

Yu, D., Tian, M., Fan, Y., Ji, G., & Wang, Y. (2012) Aggregate transitions in aqueous solutions of sodium dodecylsulfate with a "gemini-type" organic salt. *The Journal of Physical Chemistry B*, **116**: 6425–6430.

Yu, G., Jie, K., & Huang, F. (2015) Supramolecular amphiphiles based on host–guest molecular recognition motifs. *Chemical Reviews*, **115**:7240–7303.

Zha, D., & You, L. (2016) Multiresponsive dynamic covalent assemblies for the selective sensing of both Cu^{2+} and CN^{-} in water. *ACS Applied Materials & Interfaces*, **8**:2399–2405.

Zhou, L., Cheng, R., Tao, H., Ma, S., Guo, W., Meng, F., … Zhong, Z. (2011) Endosomal pH-activatable poly(ethylene oxide)-graft-doxorubicin prodrugs: Synthesis, drug release, and biodistribution in tumor-bearing mice. *Biomacromolecules*, **12**: 1460–1467.